



HAL
open science

Direct growth of III-V nanowire-based top cell for tandem on Silicon

Romaric de Lépinau, Capucine Tong, Andrea Scaccabarozzi, Fabrice Oehler, Hung-Ling Chen, Baptiste Bérenguier, Amaury Delamarre, Stéphane Collin, Andrea Cattoni

► To cite this version:

Romaric de Lépinau, Capucine Tong, Andrea Scaccabarozzi, Fabrice Oehler, Hung-Ling Chen, et al.. Direct growth of III-V nanowire-based top cell for tandem on Silicon. 2020 47th IEEE Photovoltaic Specialists Conference (PVSC), Aug 2020, Calgary (virtual), Canada. 10.1109/PVSC45281.2020.9300864 . hal-03328688

HAL Id: hal-03328688

<https://hal.science/hal-03328688>

Submitted on 30 Aug 2021

HAL is a multi-disciplinary open access archive for the deposit and dissemination of scientific research documents, whether they are published or not. The documents may come from teaching and research institutions in France or abroad, or from public or private research centers.

L'archive ouverte pluridisciplinaire **HAL**, est destinée au dépôt et à la diffusion de documents scientifiques de niveau recherche, publiés ou non, émanant des établissements d'enseignement et de recherche français ou étrangers, des laboratoires publics ou privés.

Direct growth of III-V nanowire-based top cell for tandem on Silicon

Romarc de Lépinau
Institut Photovoltaïque d'Île-de-France (IPVF)
Centre de Nanosciences et de Nanotechnologies (C2N), CNRS
Palaiseau, France
<https://orcid.org/0000-0001-9452-8380>

Capucine Tong
Institut Photovoltaïque d'Île-de-France (IPVF)
Centre de Nanosciences et de Nanotechnologies (C2N), CNRS
Palaiseau, France
capucine.tong@ipvf.fr

Andrea Scaccabarozzi
Centre de Nanosciences et de Nanotechnologies (C2N), CNRS
Palaiseau, France
andrea.scaccabarozzi@polimi.it

Fabrice Oehler
Centre de Nanosciences et de Nanotechnologies (C2N), CNRS
Palaiseau, France
fabrice.oehler@c2n.upsaclay.fr

Hung-Ling Chen
Centre de Nanosciences et de Nanotechnologies (C2N), CNRS
Palaiseau, France
<https://orcid.org/0000-0002-4260-5417>

Baptiste Berenguier
Institut Photovoltaïque d'Île-de-France (IPVF)
Palaiseau, France
baptiste.berenguier@cnrs.fr

Amaury Delamarre
Centre de Nanosciences et de Nanotechnologies (C2N), CNRS
Palaiseau, France
amaury.delamarre@c2n.upsaclay.fr

Stéphane Collin
Centre de Nanosciences et de Nanotechnologies (C2N), CNRS
Institut Photovoltaïque d'Île-de-France (IPVF)
Palaiseau, France
stephane.collin@c2n.upsaclay.fr

Andrea Cattoni
Centre de Nanosciences et de Nanotechnologies (C2N), CNRS
Institut Photovoltaïque d'Île-de-France (IPVF)
Palaiseau, France
andrea.cattoni@c2n.upsaclay.fr

Abstract— We grow and characterize solar cells based on Ga-catalyzed GaAs NWs radial p-i-n homojunctions grown by Molecular Beam Epitaxy onto inactive p-type Si(111) substrates. The solar cells feature a relatively low efficiency of 2.09% mainly due to poor $V_{oc}=0.39V$, $FF=0.4$. To assess the intrinsic quality of the GaAs NWs, we use a hyperspectral imager to determine the absolute luminescence of GaAs homojunction devices. Between 5 suns and 130 suns illumination, we find an ideality factor of 2.2 and 1.4 from J-V curves and J_{sc} -PL curves, respectively. Moreover, the quasi-Fermi level splitting ΔE_F , which represents the maximum achievable V_{oc} , is tentatively extracted from the absolute luminescence and is estimated to be above 0.8 V at 1 sun. It confirms the NWs high crystalline quality and indicates a considerable scope for improvement in device processing.

Keywords— GaAs nanowires, selective growth, Tandem on Si.

I. INTRODUCTION

The possibility to grow high structural quality III-V nanowires (NWs) on mismatched substrates such as Si, represents an elegant way to fabricate a III-V on Si tandem solar cell avoiding in one go the use of expensive III-V substrates and the difficult integration of III-V semiconductors on Si [1]. In principle, III-V NW-based top cells with an optimal bandgap at 1.7 eV can be directly grown on a Si bottom cell and efficiencies exceeding 33% at AM1.5G have been predicted for such architecture [2]. The success of this strategy relies on the precise control of the NWs growth on Si(111), their crystal structure,

doping, junction formation, passivation and opportune contacts as millions of nanometer size junctions are connected in parallel to form the NW-based solar cell. At present, state-of-the-art NW solar cells are based on axial GaAs homo-junctions with an efficiency of 15.3%. These cells are grown by MOCVD on GaAs(111)B inactive substrates using the Vapor Liquid Solid (VLS) method and a gold catalyst [3]. Ga-catalyzed GaAs NW solar cells directly grown on Si(111) stays behind, with efficiencies of 6.4% for axial homo-junction [4] and 3.3% for radial homo-junctions [5], mainly limited by relatively poor V_{oc} ($<0.39V$) and FF (<0.4).

In this work we grow and characterize Ga-catalyzed GaAs NW radial p-i-n homo-junctions grown by Molecular Beam Epitaxy (MBE) onto inactive p-type Si(111) substrates. GaAs homojunctions with AlGaAs passivation feature a relatively low efficiency 2.09% mainly due to poor $V_{oc}=0.39V$, $FF=0.4$. To assess the intrinsic quality of the GaAs NW homojunctions, we use a hyperspectral imager to determine, without contact, the absolute luminescence of the devices.

II. EXPERIMENTAL DETAILS

A. Nanowires growth

Ordered GaAs NWs are grown by MBE on p-type doped Si(111) substrates using a patterned SiO_2 mask and the Vapor-Liquid-Solid (VLS) method. A 25 nm-thick SiO_2 layer is deposited by PECVD on the Si(111) substrate and patterned

with an hexagonal array of holes (pitch 500 nm) by e-beam lithography and reactive ion etching. A 1% diluted HF solution is used to fully expose the Si(111) surface inside the nanoholes. After thermal desorption in ultra-high vacuum, the sample is transferred to the MBE chamber. The growth sequence starts with the pre-deposition of a Ga catalyst that localized only inside the holes, followed by the axial VLS growth of a short (< 20 nm) Be-doped p⁺-GaP stem and a Be-doped p-GaAs core ($L=1.8$ μm , $\phi=90$ nm). The p-GaP stem serves as a back-surface field and also to increase the yield of vertical NWs (up to 95 % over a surface area of 1.5×1.5 cm^2). The Ga droplet is consumed under an As₄ flux. An i-GaAs shell (30 nm) and a Si-doped n-GaAs shell (20 nm) are then grown by Vapor Solid method, using conditions typical of planar GaAs growth (that is supplying group V precursors in excess). The structure is finished growing a thin (10 nm) Si-doped n-AlGaAs window and a thin n-GaAs shell as contact layer. The doping concentration of the p-GaAs cores and n-type GaAs shells is measured by fitting the cathodoluminescence spectra of single NWs with the generalized Planck law [6][7][8]. The doping concentration of the p-GaAs cores corresponds to the nominal value of 3×10^{18} cm^{-3} while the doping concentration in n-GaAs shells are limited to about 5×10^{17} cm^{-3} , due to the amphoteric behavior of Si as detailed in the discussion.

B. Nanowire solar cell fabrication

The nanowire array is first coated with 50 nm SiO₂ deposit by PECVD and encapsulated in a Benzocyclobutene (BCB) by spin-coating. The excess of BCB is removed by reactive ion etching to reveal the NW heads. The SiO₂ layer is wet etched and the NW heads are then contacted using an Indium Tin Oxide (ITO) layer deposited by sputtering at ambient temperature. The electrical characteristic of the n-GaAs/ITO interface was previously studied on a planar structure as shown in Figure 1.

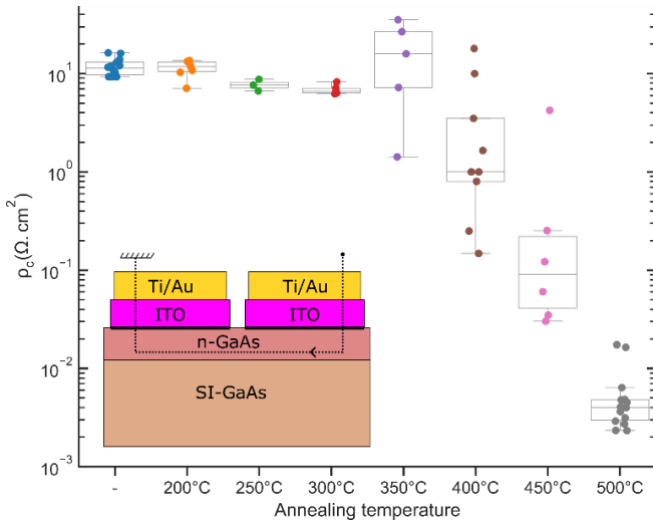


Figure 1 - Evolution of the ITO/GaAs contact resistivity with post-annealing temperature (GaAs doping $n = 1.5 \times 10^{18}$ cm^{-3} determined by Hall effect). Inset: schematic of the sample used for probing the n-GaAs/ITO interface resistivity.

The contact resistivity is relatively high and a post-annealing at $450 \div 500^\circ\text{C}$ is required to lower the contact resistivity to the $10^{-1}/10^{-2}$ Ohm cm^2 (Figure 1), which limits the voltage drop at this interface to a few tens of mV. For the device, the temperature is actually limited to 400°C to preserve the integrity of the BCB. Individual circular NW-based solar cells are finally defined by chemical etching of ITO (0.15 to 1 mm diameter) and Ti/Au annular contacts using photolithography. Figure 2a shows the cross-section SEM image of the array of GaAs p-i-n homo-junctions after planarization by BCB and ITO deposition. Figure 2b shows a SEM image of an individual diode, with ITO and metal contacts defined by photolithography.

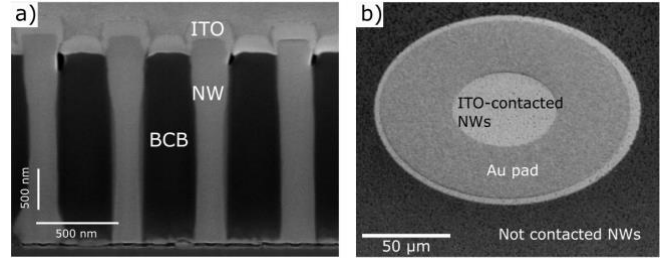


Figure 2 – a) SEM cross section of GaAs p-i-n homo-junctions after planarization and ITO deposition. b) SEM view of one NW-based diode defined by photolithography.

III. RESULTS AND DISCUSSION

Si-doped NW GaAs shells grown on the NW cores at high temperature (580°C) exhibit a good morphology (Figure 3a) but a remarkable p-type doping due to the incorporation of Si as an acceptor. Reducing the growth temperature limits the amphoteric behavior of Si thus resulting in n-type shells [9] and in fact GaAs shells grown at to 450°C show n-type doping but limited to 5×10^{17} cm^{-3} while the NW facets morphology and mask selectivity are degraded (Figure 3b).

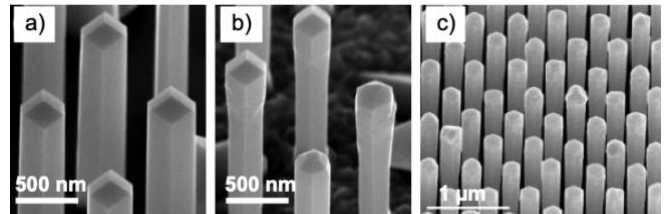


Figure 3 - SEM images of GaAs NWs homo-junctions with Si-doped shells grown at (a) 580°C and at (b) 450°C . (c) p-i-n used for the devices (before BCB planarization) with a 30 nm i-GaAs shell grown at 580°C and 20 nm p-GaAs shell grown at 450°C .

Given these constraints, we grew a 30 nm-thick i-GaAs shell at 580°C and 20 nm-thick n-GaAs shell at 450°C . The detailed sketch of the p-i-n homo-junction is shown in Figure 4.

The J-V characteristic of the NW solar cell exhibits a relatively low V_{oc} , in line with previously reported radial GaAs homo-junctions and associated with a cross-over between the dark and illuminated curves (Figure 4b). The S-shape of the illuminated

curve and the slope near $U=0V$ suggest that the device suffers from collection issues. The forward current in the dark is fitted with a one-diode model with resistances (Figure 4c) while the reverse current is high and cannot be fitted. The corresponding ideality factor is $n=4.5$, an unrealistically high value for GaAs junctions, for which idealities between 1 or 2 are expected.

Such high ideality factors typically indicate the presence of rectifying contacts (Schottky) in the structure and is consistent with the observation of collection issues from the illuminated JV curve, pointing towards unoptimized contacts.

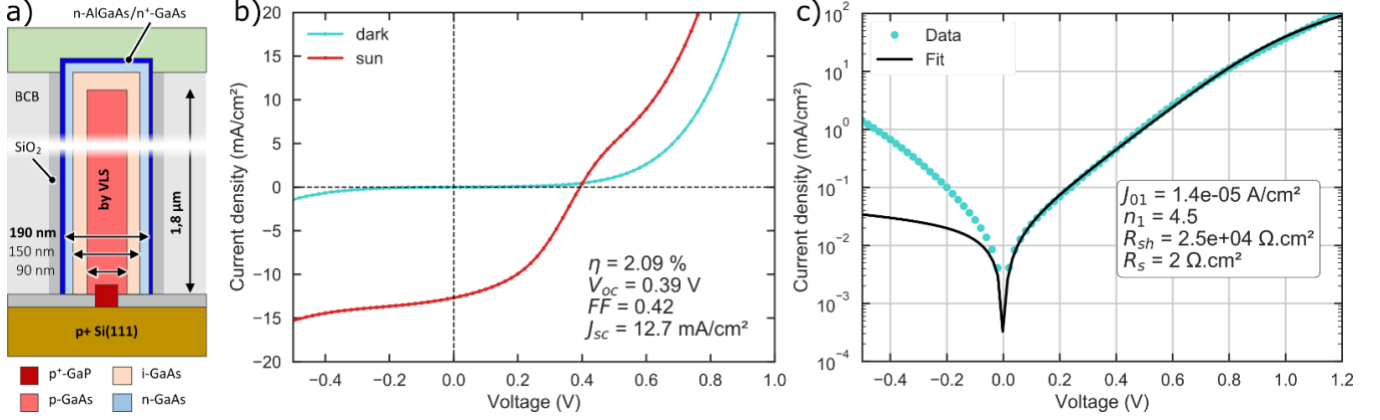


Figure 4 – a) Schematics and b) J-V (dark and 1sun) of the p-i-n GaAs homo-junction after a post-annealing (400°C) to improve the ITO/n⁺-GaAs contact. c) JV dark in logscale, along with a 1-diode fit with resistance.

To assess the intrinsic quality of the GaAs NW radial junctions, and try to understand the origin of the V_{oc} losses, we have used a hyperspectral imager to determine absolute photoluminescence (PL) in the complete devices. Luminescence emissions allow to access absorption ($A(E)$), quasi-Fermi level splitting ($\Delta\epsilon_F$) and carrier temperature (T) according to their description by the generalized Planck law [10]:

$$\Phi(E) = A(E) \frac{1}{4\pi^2 \hbar^3 c_0^2} E^2 \left[\exp\left(\frac{E - \Delta\epsilon_F}{kT}\right) - 1 \right]^{-1} \quad (1)$$

Since the hyperspectral imager allows measuring the luminescence in absolute values, the quasi-Fermi level splitting $\Delta\epsilon_F$ can be determined, which gives an indication of the intrinsic V_{oc} of the junction, without contact [11].

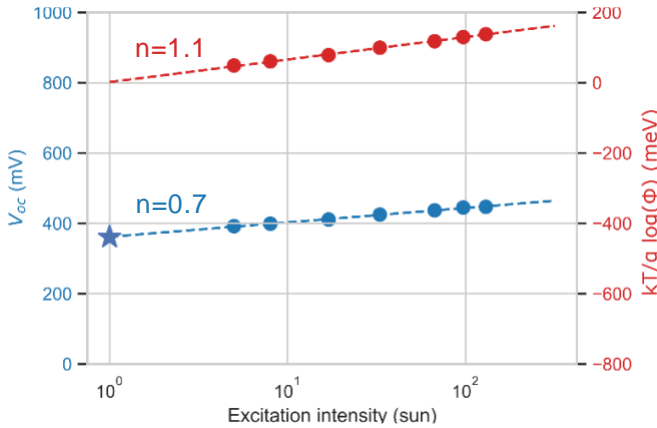


Figure 6 - Variation of the open-circuit voltage and the integrated PL under increasing illumination measured for the GaAs homo-junction.

In Figure 6 we plot the variation of the V_{oc} and the integrated luminescence under increasing illumination levels between 5 and 130 suns. An apparent ideality factor n can be extracted from the power law:

$$V_{oc} = \frac{nkT}{q_0} \log\left(\frac{J_{sc}}{J_0}\right) \quad (2)$$

We find $n=0.7$, a much lower value than the one extracted from the experimental J-V curve ($n=4.5$) of Figure 4c. Using Eq. (1), the variations of the quasi-Fermi level splitting $\Delta\epsilon_F$ can be approximated by $kT \times \log(\Phi)$ plotted in red in Figure 6 for different illuminations intensities, and an ideality factor can be extracted similarly. We find $n=1.1$, which is consistent with ideality factors expected for GaAs junctions. The precise extraction of the quasi-Fermi level splitting values from the PL spectra is complicated by the presence, in the PL spectra, of a broadening probably due to the PL emission from the AlGaAs shell or the ITO. The hyperspectral characterization of other samples before and after the planarization and ITO deposition is currently in progress in order to discriminate the possible contribution of the AlGaAs shell or the ITO to the spectral line shape. However, a preliminary analysis gives $\Delta\epsilon_F=0.91\text{ V}$ at 5 suns, extrapolated to $\Delta\epsilon_F=0.86\text{ V}$ at 1 sun, which represents the maximum achievable V_{oc} , while the actual V_{oc} reaches only 0.39 mV. It confirms the high crystalline quality of the NWs and indicates a considerable scope for improvement in device processing.

IV. CONCLUSION

We fabricated and characterize NWs based GaAs homo-junctions. While the devices feature relatively low efficiencies, hyperspectral imaging reveals the intrinsic high quality of the homo-junctions: this is an encouraging information for the community working on NWs-based solar cells and we expect that better V_{oc} and FF should result from improved device processing (possibly GaAs/ITO contact).

ACKNOWLEDGMENT

This work was partially funded by the ANR Project NANOCELL, (ANR-15-CE05-0026).

REFERENCES

- [1] M. Feifel, et al., « Direct Growth of III–V/Silicon Triple-Junction Solar Cells With 19.7% Efficiency », *IEEE J. Photovoltaics* 8, 1590 (2018).
- [2] R.R. LaPierre, « Theoretical conversion efficiency of a two-junction III–V nanowire on Si solar cell », *J. Appl. Phys.*, 110, 014310 (2011).
- [3] I. Aberg, et al., « A GaAs Nanowire Array Solar Cell With 15.3% Efficiency at 1 Sun », *IEEE J. Photovoltaics* 6, 185 (2016).
- [4] M. Yao et al., « Tandem Solar Cells Using GaAs Nanowires on Si: Design, Fabrication, and Observation of Voltage Addition », *Nano Lett.*, 15, 7217 (2015).
- [5] J.P. Boulanger, et al., « Characterization of a Ga-Assisted GaAs Nanowire Array Solar Cell on Si Substrate », *IEEE J. Photovoltaics*. 6, 661 (2016).
- [6] H.-L. Chen et al., « Determination of n-Type Doping Level in Single GaAs Nanowires by Cathodoluminescence », *Nano Letters* 17, 6667 (2017).
- [7] H.-L. Chen et al., « Quantitative Assessment of Carrier Density by Cathodoluminescence (1): GaAs thin films and modeling », *arXiv:1909.05598*.
- [8] H.-L. Chen et al., « Quantitative Assessment of Carrier Density by Cathodoluminescence (2): GaAs nanowires », *arXiv:1909.05602*.
- [9] E.S. Tok, et al., « Growth of Si-doped GaAs(110) thin films by molecular beam epitaxy; Si site occupation and the role of arsenic », *J. Appl. Phys.*, 83, 4160 (1998).
- [10] P. Würfel, « The chemical potential of radiation », *J. Phys. C: Solid State Phys.* 15, 3967 (1982).
- [11] A. Delamarre et al., « Characterization of solar cells using electroluminescence and photoluminescence hyperspectral images », *Journal of Photonics for Energy* 2, 027004 (2012).